Journal of Biomedical Optics

BiomedicalOptics.SPIEDigitalLibrary.org

Bacteriophage-mediated identification of bacteria using photoacoustic flow cytometry

Robert H. Edgar
Justin Cook
Cierra Noel
Austin Minard
Andrea Sajewski
Matthew Fitzpatrick
Rachel Fernandez
John D. Hempel
John A. Kellum
John A. Viator

SPIE.

Robert H. Edgar, Justin Cook, Cierra Noel, Austin Minard, Andrea Sajewski, Matthew Fitzpatrick, Rachel Fernandez, John D. Hempel, John A. Kellum, John A. Viator, "Bacteriophage-mediated identification of bacteria using photoacoustic flow cytometry," *J. Biomed. Opt.* **24**(11), 115003 (2019), doi: 10.1117/1.JBO.24.11.115003.

Bacteriophage-mediated identification of bacteria using photoacoustic flow cytometry

Robert H. Edgar,[a] Justin Cook,[b] Cierra Noel,[b] Austin Minard,[b] Andrea Sajewski,[b] Matthew Fitzpatrick,[b] Rachel Fernandez,[b] John D. Hempel,[b] John A. Kellum,[c] and John A. Viator[a,b,*]
[a]University of Pittsburgh, Swanson School of Engineering, Department of Bioengineering, Pittsburgh, Pennsylvania, United States
[b]Duquesne University, Pittsburgh, Pennsylvania, United States
[c]University of Pittsburgh, Center for Critical Care Nephrology, Department of Critical Care Medicine, Pittsburgh, Pennsylvania, United States

Abstract. Infection with resistant bacteria has become an ever increasing problem in modern medical practice. Currently, broad spectrum antibiotics are prescribed until bacteria can be identified through blood cultures, a process that can take two to three days and is unable to provide quantitative information. To detect and quantify bacteria rapidly in blood samples, we designed a method using labeled bacteriophage in conjunction with photoacoustic flow cytometry (PAFC). PAFC is the generation of ultrasonic waves created by the absorption of laser light in particles under flow. Bacteriophage is a virus that infects bacteria and possesses the ability to discriminate bacterial surface antigens, allowing the bacteriophage to bind only to their target bacteria. Bacteria can be tagged with dyed phage and processed through a photoacoustic flow cytometer where they are detected by the acoustic response. We demonstrate that *E. coli* can be detected and discriminated from *Salmonella* using this method. Our goal is to develop a method to determine bacterial content in blood samples. We hope to develop this technology into future clinical use and decrease the time required to identify bacterial species from 3 to 4 days to less than 1 hour. [DOI: 10.1117/1.JBO.24.11.115003]

Keywords: diagnostics; optoacoustics; bacteriophage.

Paper 190266R received Aug. 1, 2019; accepted for publication Nov. 4, 2019; published online Nov. 22, 2019.

1 Introduction

Bacterial infections that may lead to sepsis in patients is a major problem in many aspects of hospital care, including emergency medicine, transplant surgery, and intensive care.[1] To combat these infections, current medical practice calls for the use of broad spectrum antibiotics until bacterial cultures can identify specific pathogens. Because of the doubling time of bacteria, this process may take 48 to 96 h. There are also well-known drawbacks to broad spectrum antibiotic use, such as increased antibiotic resistance, costs, and toxicity.[2] Furthermore, some outbreaks involve bacteria that are resistant to standard broad spectrum coverage, and delays in diagnosis may result in more advanced disease.

Bacterial cultures are still the gold standard for identification of blood stream infections,[3] though there is a critical need to develop early detection and identification methods for bacterial pathogens that avoid the requirement of bacterial culture, obviate the need for broad spectrum antibiotics, and improve patient outcomes.[4]

As an early diagnostic tool, Gram staining, developed in the 19th century, is employed to narrow the types of possible bacteria before culture results can be obtained. Gram staining allows doctors to group bacteria into classes correlated with likely antibiotic sensitivity 24 h before bacteria can be identified from plate cultures.[5] However, this method classifies thousands of bacterial strains, pathologic or not, into four large groups and is incapable of providing further resolution. Thus, a variety of newer assays have been developed in an effort to obtain faster bacterial identification. Many of these assays detect bacterial DNA and require polymerase chain reaction (PCR).[6–8]

Clinical PCR assays, unlike in research laboratory settings, have to deal with secondary and tertiary DNA structures, unknown salt content, and additional polymerase inhibitors such as ethylenediaminetetraacetic acid (EDTA) and immunoglobulins.[9] FDA cleared pneumonia pathogen test by Unyvero is a qualitative multiplex PCR that has been widely used but has a higher limit of detection (1×10^4 to 1×10^5 CFU/ml) due to traditional respiratory culture (1×10^3 CFU/ml).[10] The most widely adopted rapid diagnostic tests, Verigene and FilmArray, as well as the majority of available rapid diagnostic tests, require amplification of the organism from inoculated blood culture broth.[10] Microarrays and real-time PCR have been developed, which produce more consistent results but can be cost prohibitive.[11] Furthermore, because of the amplification, the techniques are only semiquantitative. Approaches that obviate the need for DNA amplification, such as smudge plate in conjunction with matrix-assisted laser desorption ionization time-of-flight (MALDI-TOF) identification, still require 19 h of culture and growth time before identification.[12] Implementation of MALDI-TOF systems nearly halved the amount of time to optimal antibiotic therapy (63 versus 32 h) but still required more than the desired time to optimal therapy.[13] T2 Biosystems tests, based on magnetic resonance, do not require positive cultures, but do require expensive and sensitive machinery and deliver results in 3 to 6 h.[14] Using *in-situ* hybridization, the PhenoTest BC can deliver results in 90 min and produce antimicrobial susceptibility testing in 7 h. The PhenoTest BC has sensitivity of 94.6% and a very major error rate of 1% when tested in a multicenter evaluation.[15] Each of these rapid diagnostic systems has advanced therapeutic care and decreased the time to prescription of targeted antibiotics.

*Address all correspondence to John A. Viator, E-mail: viatorj@duq.edu

A promising candidate technology for advancing therapeutic care when dealing with bacterial identification is photoacoustic flow cytometry (PAFC), which can find rare particles in fluids using the photoacoustic effect.[16] PAFC is not a new technology and has been utilized by several groups. Zharov et al.[17] have detected particles under flow in mouse blood vessels by labeling with carbon nanotubes or gold nanorods. PAFC systems have been used to target *Staphylococcus aureus* cells labeled using antibody-fused gold nanoparticles.[18] Other groups expanded on this work to develop photoacoustic detection coupled with photothermal eradication of bacteria *in vivo* model.[19] More recently, *in vivo* photoacoustics have been used with magnetotactic bacteria as well as the detection of infected phagocytic macrophage cells through a novel interaction and self-assembly.[20,21] In contrast, our method uses a bacterial tag, bacteriophage that binds irreversibly and specifically, and does not require a bacterial culture step or DNA amplification, such as many clinical diagnostics. Accuracy can be achieved by leveraging bacteriophage that binds to bacteria irreversibly and with specificity,[22] including to subspecies, often correlating with antibiotic sensitivity patterns. Bacteriophage can be modified to optically create absorbing bacterial tags. By exploiting the different host ranges of bacteriophage, we are able to further discriminate pathogenic bacterial strains from nonpathogenic strains. Bacteriophages present many advantages over antibodies or other types of tags. Bacteriophages have greater specificity than antibodies, are easier to produce, bind irreversibly, and are more stable.[23–26] Bacteriophages are able to identify and discriminate target bacteria within a matter of seconds, even in complex environments such as blood.[27] Bacteriophage host attachment is determined by tail spike, or long tail fiber, proteins attached to the distal end of their tail structure.[28] These specialized bacteriophage proteins have evolved to bind to bacterial surface antigens that are essential to the bacteria and thus are not easily changed. Additionally, the majority of bacteriophages have multiple tail spike trimers or long tail fibers, all of which allow the bacteriophage binding to be fast, specific, and irreversible.[23] Tail fiber and tail spike proteins, essential to the survival and fitness of bacteriophage, have developed to be the most stable protein structures yet to be discovered. As bacteria have continued to evolve and diverge, bacteriophages have coevolved and adapted to infect new and different subspecies of bacteria, even those bacteria that have acquired antibiotic resistance. Bacterial virulence is always accompanied by changes in cell surface antigens, and bacteriophages often take advantage of this fitness cost by target virulence factors and essential genes.[29] The ability of bacteriophage to discriminately and irreversibly bind to their target bacteria is central to their evolutionary fitness and survival.

In this study, we use bacteriophage Det7 and bacterial strains LT2 *Salmonella* and K12 *E. coli* (Fig. 1). The genome of bacteriophage Det7, the particle structure, and the host range have previously been characterized.[28,30] Det7 bacteriophage binds specifically to the O-antigen of many *Salmonella* strains but does not bind to any *E. coli* strains. *Salmonella* and *E. coli* were used because of their physical similarities, the diversity of surface antigens, and the host of literature using them as model organisms for bacterial identification.[31]

2 Materials and Methods

PAFC generates ultrasonic waves resulting from absorption of light in particles under flow.[32] These ultrasonic waves are often created by thermoelastic expansion and contraction of an object that absorbed laser light.[33,34] In our PAFC setup, a nanosecond laser operating at 532 nm is used to irradiate a sample under flow. The ultrasonic waves are detected by a piezoelectric transducer and recorded onto a computer. Our photoacoustic sensing setup is directly based on our system used to detect circulating melanoma cells in blood.[35–37]

Bacteriophages have low optical absorbance at 532-nm wavelength. To provide optical contrast to bacteriophage Det7, Direct Red 81 dye, a polysulfated photostable protein dye capable of generating photoacoustic waves after laser irradiation, was attached. Absorption spectra of dyed and undyed bacteriophage Det7 were measured using a Nanodrop 2300. Bacteriophage remains permanently dyed by Direct Red 81, which contains two sulfonic acid groups with pKa values in the negative range, allowing salt bridges to form with basic groups such as lysine and arginine side chains. These salt bridges are more tenacious than some covalent bonds at relatively neutral pH values, and therefore, these bonds are only broken at an elevated pH in high salt concentrations.

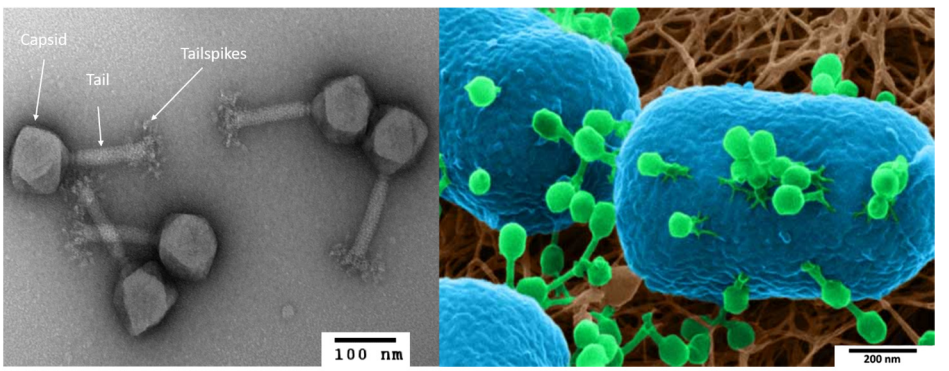

Fig. 1 (a) Electron micrographs of bacteriophage Det7 showing the major structural components of all bacteriophage. Micrograph taken on a FEI Morggagni TEM by Edgar. (b) Multiple bacteriophage particles attached to a single *E. coli* cell imaged using helium ion microscopy by Leppänen et al.[38] (image used with permission from Wiley).

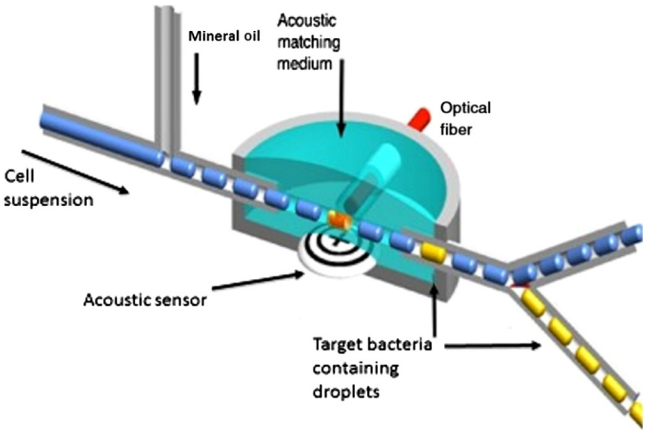

Fig. 2 Schematic of photoacoustic flow chamber with parts labeled for identification.

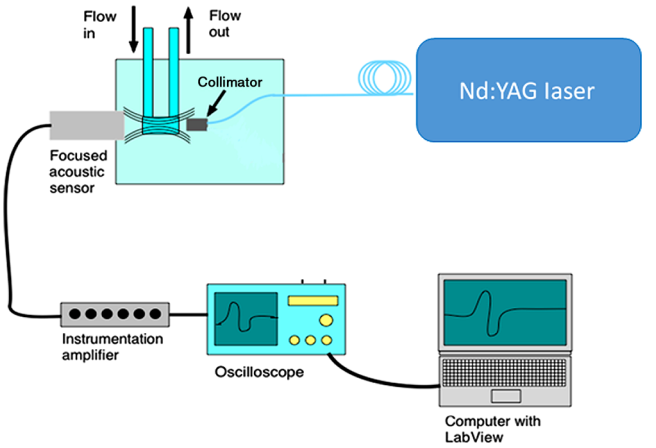

Fig. 3 Schematic of photoacoustic flow setup with parts labeled for identification.

2.1 *Photoacoustic Flow Cytometry*

A Nd:YAG laser (Litron Nano, Bozeman, Montana) coupled into a 1000 μm, 0.39 numerical aperture, optical fiber (Thorlabs, Newton, New Jersey) was used to produce 532-nm laser light with 5-ns pulses. The laser beam energy coupled through the optical fiber was maintained and measured from 1.9 to 2.1 mJ for most detection experiments. Laser energy was increased to 4 mJ for single cell detection experiment. Laser light was directed to a quartz tube (Quartz 10 QZ, Charles Supper, Natick, Massachusetts) with 10-μm-thick walls passing through a 3D-printed flow chamber. The 10-μm-thick walls allow the propagation of ultrasonic waves, as well as providing an optically transparent pathway for the sample to flow through. Optical fiber was placed 5 mm from the quartz tube to create a detection volume of 0.04 μl. Laser beam shape was Gaussian and fluence was calculated to be 0.014 mJ/cm^2.

A 2.25-MHz transducer focused on the quartz sample tube was fitted to the base of the 3D-printed flow chamber (Fig. 2). The internal volume of the chamber was filled with Sonotech LithoClear acoustic gel (NeXT Medical Products Company, Branchburg, New Jersey) to provide a medium for the propagation of acoustic waves. Syringe pumps were used to create an alternating flow of sample and mineral oil equal to 60/min flow rate. The introduction of sample and the immiscible mineral oil induced two-phase flow.[37] Two-phase flow was employed to allow for future collection of the samples for further analysis while eliminating the possibility of samples becoming stuck or delayed inside the tubing. Signals were amplified with a gain of 50 using a Tegam 4040B amplifier (Tegam, Inc., Geneva, Ohio) and sent to a desktop computer running a customized LabView program. This computer also served for system control and data collection. This flow chamber setup served as the excitation and acoustic wave collection device.

Detections were determined by two methods. Primary detection was through amplitude detection above a given threshold. Threshold was empirically set at 1.5 times the root-mean-square noise value. A scoring function derived from known positive detections was derived to score each waveform based on its key aspects. Each detection above threshold was scored using the scoring function and given a confidence value (Fig. 3).

2.2 *Bacteriophage Preparation*

Det7 bacteriophage lysates were concentrated using polyethylene glycol 8000 precipitation described by Castro-Mejía et al.[39] and initially described by Yamamoto et al.[40] Differential centrifugation and cesium chloride gradients were used to further purify and concentrate bacteriophage Det7 stocks.[41] Stock concentrations of 5×10^{11} plaque forming units per milliliter (PFU/ml) or greater were produced. Pure stocks of bacteriophage were then diluted into a saturated solution of Direct Red 81 dye (Sigma Aldrich, Saint Louis, Missouri). Bacteriophage Det7 virion particles were then pelleted and resuspended in 10 mM Tris, pH 7.5, 10 mM $MgCl_2$, 68 mM NaCl (bacteriophage buffer) to remove any unbound dye. A NanoDrop 2300 spectrophotometer was used to record the absorbance spectrum and to verify an increase in dyed bacteriophage absorbance at 532-nm wavelength. An increase of absorbance at 532 nm was identified for dyed bacteriophage Det7 when compared to the absorbance of undyed Det7 bacteriophage. Dyed Det7 bacteriophages were retested for their ability to infect their target bacteria and stocks were titered to determine the total number of dyed infectious particles. Titers before and after dyeing protocol are expected to be within 3% to 5%, as this is the expected variation derived from multiple titers. Any decrease in titer would suggest that the dye modification is inactivating bacteriophage particles. No difference in titer was determined even when Det7 bacteriophages were kept in an excess of dye for 60 days, demonstrating that the bacteriophages are robust and unaffected by the attachment of the Direct Red 81 dye.

3 Results

3.1 *Bacteriophage Detection*

Bacteriophage buffer was run through the PAFC system to demonstrate a level of background detection and any variability with PBS. Purified bacteriophages were next titered through the PAFC system; 0.5 ml of each concentration ranging from 1×10^1 PFU/ml to 1×10^{12} PFU/ml were tested. No detections were observed for either undyed bacteriophages or phage buffer, demonstrating their inability to absorb laser light and produce a photoacoustic response using 2-mJ laser energy.

Next, purified dyed bacteriophages were tested with a laser energy of 2 mJ; 0.5 ml of each concentration ranging from

Table 1 Detection of bacteria, bacteriophage, and dyed bacteriophage.

	Concentration	Detections
Salmonella LT2	10^1 to 10^8	0
E. coli K12	10^1 to 10^8	0
Undyed bacteriophage	10^1 to 10^{12}	0
Dyed bacteriophage	10^1 to 10^{10}	0
Dyed bacteriophage	10^{11} to 10^{12}	873 to 915

1×10^1 PFU/ml to 1×10^{12} PFU/ml were tested. As can be seen in Table 1, no detections were recorded until bacteriophages reached a concentration of 1×10^{11} PFU/ml. At a concentration of 1×10^{11} PFU/ml, there are $\sim 1 \times 10^5$ dyed bacteriophages in the detection volume of 0.04 μl. Using 2 mJ of laser energy, 1×10^5 dyed bacteriophages per detection volume produce a signal that crosses our threshold of 1.5 times the root-mean-square noise value. All concentrations below 1×10^{10} PFU/ml bacteriophage were assumed to be free-floating and evenly dispersed throughout the sample (Fig. 4).

3.2 *Bacterial Detection*

The photoacoustic response of free-floating bacteria was determined next. Overnight cultures of *Salmonella* LT2 and *E. coli* K12 were grown and diluted into fresh LB media. Cultures were grown at 37°C for 3 h to ensure bacteria were in exponential growth phase. Dilutions of each exponential culture were made and concentrations from 1×10^8 CFU/ml through 1×10^1 CFU/ml were tested for their photoacoustic response. Neither *Salmonella* LT2 nor *E. coli* K12 produced a photoacoustic response and no detections were recorded.

After determining background and baseline detection thresholds, we turned our attention toward our goal of detecting bacteria. When bacteriophages bind to their target bacteria, they are localized on the cell surface. This localization of bacteriophages, even when total concentration is well below detectable concentrations, creates a local increase in concentration that is then above the detection threshold. It is this localization of bacteriophages that results in the production of signals above our detection threshold.

Table 2 Detection of target bacteria.

Bacteria	Dyed bacteriophage	Ratio	Detections
Salmonella LT2 10^5 CFU/ml	Det7 10^5 PFU/ml	1:1	0
Salmonella LT2 10^5 CFU/ml	Det7 10^6 PFU/ml	1:10	0
Salmonella LT2 10^5 CFU/ml	Det7 10^7 PFU/ml	1:100	2
Salmonella LT2 10^5 CFU/ml	Det7 10^7 PFU/ml	1:1000	496
Salmonella LT2 10^6 CFU/ml	Det7 10^8 PFU/ml	1:1000	55
Salmonella LT2 10^7 CFU/ml	Det7 10^9 PFU/ml	1:1000	83
Salmonella LT2 10^8 CFU/ml	Det7 10^{11} PFU/ml	1:1000	502

Bacteriophage Det7 dyed with Direct Red 81 was incubated with *Salmonella* LT2 or *E. coli* K12 and allowed to bind to the bacterial cell surface. The host range of Det7 has previously been tested and described in detail.[28] Det7 infects a wide variety of *Salmonella* serovars but does not infect any *E. coli* strains. *Salmonella* LT2 bacteria were incubated with dyed Det7 bacteriophage in increasing ratios from 1:1 (bacteria:bacteriophage) increasing by order of magnitude to 1:1000. Mixed cultures were held at room temperature for 10 min to allow the bacteriophage time to adsorb to the surface of the *Salmonella* cells. Tests were run with bacterial cell concentrations ranging from 1×10^4 CFU/ml to 1×10^8 CFU/ml. Each test was repeated using target bacteria, *Salmonella* LT2, and nontarget bacteria, *E. coli* K12. Table 2 demonstrates that in the presence of target bacteria, *Salmonella* LT2, and below threshold concentrations of dyed bacteriophage, Det7, multiple detections were recorded. Detections were limited with a built-in delay between signals to allow recording of each waveform. This delay limited the total number of signals that could be detected to 660 signals per test.

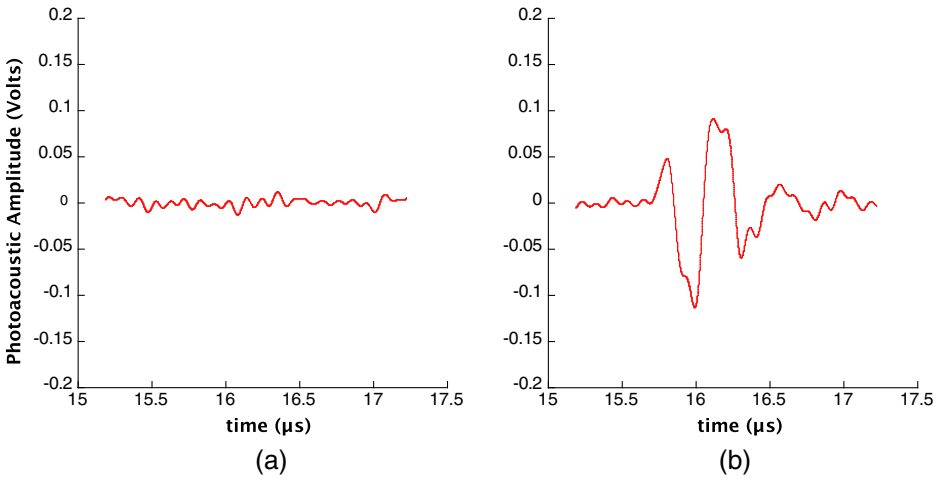

Fig. 4 (a) Signal from irradiating PBS, resulting in background noise. (b) Signal generated from irradiating bacteriophage bound to target bacteria. A detection is defined as any single waveform with 1.5 times or greater amplitude than the root-mean-square noise value.

Table 3 Detection of nontarget bacteria.

Bacteria	Dyed bacteriophage	Ratio	Detections
E. coli K12 10^8 CFU/ml	Det7 10^{11} PFU/ml	1:1000	3
E. coli K12 10^7 CFU/ml	Det7 10^{10} PFU/ml	1:1000	0
E. coli K12 10^6 CFU/ml	Det7 10^9 PFU/ml	1:1000	0
E. coli K12 10^5 CFU/ml	Det7 10^8 PFU/ml	1:1000	0
E. coli K12 10^4 CFU/ml	Det7 10^7 PFU/ml	1:1000	0

Table 4 Single cell detection.

Laser energy (mJ)	LT2:Det7 ratio	Expected	Detected
4	1:1000	100	58
4	1:1000	100	32
4	1:1000	100	31
4	1:1000	100	41
4	1:1000	100	55

Both the 1×10^4 CFU/ml and 1×10^8 CFU/ml were near constant detections, and the 1×10^5 CFU/ml and 1×10^6 CFU/ml showed a much lower number of detections. Table 3 shows that for nontarget, *E. coli* K12, no detections were recorded when mixed with dyed Det7 bacteriophage, except at a concentration of dyed bacteriophage of 1×10^{11} PFU/ml. At a concentration of 1×10^{11} PFU/ml, there are 1×10^6 bacteriophages per detection volume of 0.04 μl.

We next directed our attention toward our goal of detecting single bacterial cells tagged with labeled bacteriophage. LT2 *Salmonella* was mixed with dyed Det7 bacteriophages in a 1:1000 ratio. The cell/bacteriophage mixtures were serially diluted to produce 100 cells per test volume of 0.5 ml and laser energy was increased to 4 mJ. The experiment was replicated 5 times with new serial dilutions of bacterial cells and bacteriophages to ensure the significance of detection numbers. As seen in Table 4, we detected an average of 43.4 out of every one hundred cells.

4 Discussion

4.1 *Bacteriophage Detection*

Undyed bacteriophage showed no photoacoustic response when run through our detection system. When Direct Red 81 dye was added to the phage particles, detections were only observed when concentrations of phage reached 1×10^{11} PFU/ml. At a concentration of 1×10^{11} PFU/ml, there will be $\sim 4 \times 10^5$ dyed bacteriophages per detection volume of 0.04 μl, resulting in a signal. At a concentration of 1×10^{10} PFU/ml, bacteriophages are present at about the level of one bacteriophage per 0.6 μm^3, which is about the volume of a bacterial cell. We hypothesize that at 1×10^{11} PFU/ml concentration, bacteriophages start to clump together and form multiphage complexes, as has previously been seen by electron microscopy. Multiphage complexes can form for a variety of reasons, chief among them would likely be entanglement of tail fibers or low pH as described by Goldwasser et al.[42] All concentrations of bacteriophages below 1×10^{11} PFU/ml are assumed to be free-floating and evenly distributed. Free-floating bacteriophages less than $\sim 4 \times 10^5$ per detection volume are below the detection threshold for our system. A signal is produced when target bacteria are present that allow bacteriophage binding. Binding of multiple bacteriophages to a bacterial cell surface will increase the local concentration of dyed bacteriophage. We hypothesize that this increase in local concentration of bacteriophages is what leads to a positive signal above our detection threshold.

4.2 *Bacterial Detection*

Tables 2 and 3 demonstrate that our bacteriophages are specific to their target bacteria and that we do not get a signal from unattached bacteriophages except when in extremely high concentrations. Table 2 shows our ability to detect bacterial cells when tagged with dyed bacteriophages. When cells are tagged with 1, 10, or 100 bacteriophages, they are below our detection threshold. Some cells were missed due to our built-in delay for recording of signals while others were simply missed due to our testing of only a single laser energy. In Table 2, the concentrations of bacteria with 1000 bacteriophages per cell showed detections. Due to our built-in delay, 1×10^5 CFU/ml and 1×10^8 CFU/ml showed saturated detections. Laser energies of 4 mJ have previously been shown to increase detection sensitivity of the system. In future trials, increasing laser energies will be tested until our background noise increases or we reach 100% cell detections. The variation between the number of detections between the 1×10^4 CFU/ml and 1×10^8 CFU/ml and 1×10^5 CFU/ml and 1×10^6 CFU/ml could be due in part to nonhomogeneous mixing of our bacteria and phage. Additionally, there could have been imperfections or bubbles in our acoustic gel that led to decreased signal propagation. Additional work is being done to remove bubbles from acoustic gel and develop better and more permanent ways of producing flow chambers and ensuring acoustic coupling in our system. Currently, repeated measurements in alternating orders are used to rectify this inconsistency. This represents an area of refinement and future work in preparing this system for more diagnostic purposes. Table 4 demonstrates our system's ability to detect individual cells when tagged with modified bacteriophage. Cells were serially diluted to produce roughly 100 cells per test volume. Chase and Hoel[43] first described and modeled the error associated with serial dilutions of bacteria and bacteriophage. We therefore expect some variation and loss of cells from manual pipetting and serial dilutions. Despite this loss, we detected nearly 50% of estimated cells. Future work to resolve this challenge and produce 100% detection rate will come from using higher concentrations of cells with less chance of loss as well as optimizing our flow system. Using higher concentrations of bacteria will reduce the error from pipetting and serial dilutions. In future trials, bacteria can be collected after exiting our flow system and plated to determine relative number of bacteria present and calculate loss. Additionally, larger sample sizes will provide more robust measurements and greater accuracy in number of bacteria present. Moreover, the ability to detect about half of all single cells is probably much more sensitive than needed clinically, as the concentration of bacteria in blood would need to be much higher to cause illness in a human being.

4.3 *Conclusion*

Bacteriophages have evolved to identify and bind to their target bacteria with high specificity. Bacteriophage host attachment is mediated solely by tail fibers.[28] Tail fibers are differentiated into long tail fibers, such as bacteriophage T4, and tail spike proteins, such as P22 TSP. Bacteriophage host attachment has many advantages over antibodies. Antigens used by antibodies are often the most abundant surface molecules or those that cause the greatest immune response.[44] These surface molecules can often change to avoid antibody detection.[45] Conversely, bacteriophages have evolved to use surface epitopes that are essential and difficult to change.[46] Bacteriophages have even been shown to target cell surface pumps used in bacterial antibiotic resistance. Though bacteriophage resistance can evolve, it happens at a much lower rate than antibody avoidance and always has a negative fitness effect on the bacteria.[47] Bacteriophage attachment proteins are also among the most stable protein structures to be discovered and bind the phage irreversibly to the bacterial cell.[48] Antibodies are more expensive to produce,[49] are less stable,[50] and bind less strongly than bacteriophages. Antibodies have a binding constant, kD, in the range of 1 to 10 nM while bacteriophages have a binding constant closer to 10 to 50 nM.[51,52]

PAFC presents a rapid way to detect microscopic particles under flow based on their ability to absorb laser light. These initial experiments demonstrate our ability to use readily available protein dyes on bacteriophages without affecting their ability to attach to target bacteria. This research presents an innovative way of identifying and differentiating bacterial strains. This method can be further developed for use with other bacterial pathogens in blood cultures, representing a major step forward in clinical practice. The time and money saving potential of rapid detection and identification of bacterial infection are overshadowed only by the number of potential lives saved. Often the limiting factors for treatment of patients is the time spent waiting for results. It is our hope that the work presented above can be a foundation for future work and an ability to detect bacterial pathogens in blood cultures. Bacterial plate cultures and Gram staining are 19th-century technologies that have been the gold standard for decades, but current trends in resistant bacteria have necessitated a move toward more rapid and quantifiable diagnostic tools.

Disclosures

R. H. Edgar, J. D. Hempel, J. A. Kellum, and J. A. Viator have interest in PhotoPhage Systems, LLC, a company formed to commercialize photoacoustic technologies.

Acknowledgments

The research reported in this article was supported by the National Cancer Institute of the U.S. National Institutes of Health under Award No. 1R01CA161367-01.

References

1. C. L. Ventola, "The antibiotic resistance crisis: part 1: causes and threats," *Pharm. Ther.* **40**(4), 277 (2015).
2. B. L. Bearson and B. W. Brunelle, "Fluoroquinolone induction of phage-mediated gene transfer in multidrug-resistant *Salmonella*," *Int. J. Antimicrob. Agents* **46**(2), 201–204 (2015).
3. N. Mancini et al., "The era of molecular and other non-culture-based methods in diagnosis of sepsis," *Clin. Microbiol. Rev.* **23**(1), 235–251 (2010).
4. M. H. Kollef, "Broad-spectrum antimicrobials and the treatment of serious bacterial infections: getting it right up front," *Clin. Infect. Dis.* **47**(Suppl. 1), S3–S13 (2008).
5. X.-G. Guo and Q.-F. Liu, "Gram stain and molecular method for the diagnosis of bacterial pneumonia," *Chin. Med. J.* **129**(15), 1884 (2016).
6. A.-K. Järvinen et al., "Rapid identification of bacterial pathogens using a PCR- and microarray-based assay," *BMC Microbiol.* **9**(1), 161 (2009).
7. H. Won et al., "Rapid identification of bacterial pathogens in positive blood culture bottles by use of a broad-based PCR assay coupled with high-resolution melt analysis," *J. Clin. Microbiol.* **48**(9), 3410–3413 (2010).
8. Y.-T. Chang et al., "Rapid identification of bacteria and *Candida* pathogens in peritoneal dialysis effluent from patients with peritoneal dialysis-related peritonitis by use of multilocus PCR coupled with electrospray ionization mass spectrometry," *J. Clin. Microbiol.* **52**(4), 1217–1219 (2014).
9. W. A. Al-Soud and P. Rådström, "Purification and characterization of PCR-inhibitory components in blood cells," *J. Clin. Microbiol.* **39**(2), 485–493 (2001).
10. K. V. Sullivan and J. D. Bard, "New and novel rapid diagnostics that are impacting infection prevention and antimicrobial stewardship," *Curr. Opin. Infect. Dis.* **32**(4), 356–364 (2019).
11. K. Murai et al., "Cost-effectiveness of diagnostic strategies using quantitative real-time PCR and bacterial culture to identify contagious mastitis cases in large dairy herds," *Prev. Vet. Med.* **113**(4), 522–535 (2014).
12. Y. Chen et al., "Rapid identification of bacteria directly from positive blood cultures by use of a serum separator tube, smudge plate preparation, and matrix-assisted laser desorption ionization-time of flight mass spectrometry," *J. Clin. Microbiol.* **53**(10), 3349–3352 (2015).
13. A. M. P. Kratz, K. V. Sullivan, and J. C. Gallagher, "Clinical impact of matrix-assisted laser desorption ionization time-of-flight mass spectrometry for the management of inpatient pneumonia without additional antimicrobial stewardship support," *Infect. Control Hosp. Epidemiol.* **40**(9), 1053–1055 (2019).
14. B. Manning et al., "Automated detection of *Candida auris* direct from whole blood by T2MR," *Open Forum Infect. Dis.* **4**(Suppl. 1), S609–S610 (2017).
15. P. Pancholi et al., "Multicenter evaluation of the accelerate phenotest BC kit for rapid identification and phenotypic antimicrobial susceptibility testing using morphokinetic cellular analysis," *J. Clin. Microbiol.* **56**(4), e01329-17 (2018).
16. R. Edgar et al., "Identification of MRSA infection in blood using photoacoustic flow cytometry," *Proc. SPIE* **10878**, 1087860 (2019).
17. V. P. Zharov et al., "Photoacoustic flow cytometry: principle and application for real-time detection of circulating single nanoparticles, pathogens, and contrast dyes *in vivo*," *J. Biomed. Opt.* **12**(5), 051503 (2007).
18. N. J. Millenbaugh et al., "Photothermal killing of *Staphylococcus aureus* using antibody-targeted gold nanoparticles," *Int. J. Nanomed.* **10**, 1953 (2015).
19. E. I. Galanzha et al., "*In vivo* magnetic enrichment, photoacoustic diagnosis, and photothermal purging of infected blood using multifunctional gold and magnetic nanoparticles," *PLoS One* **7**(9), e45557 (2012).
20. Z. A. Nima et al., "Bioinspired magnetic nanoparticles as multimodal photoacoustic, photothermal and photomechanical contrast agents," *Sci. Rep.* **9**(1), 887 (2019).
21. Q. Cai et al., "Chemotaxis-instructed intracellular *Staphylococcus aureus* infection detection by a targeting and self-assembly signal-enhanced photoacoustic probe," *Nano Lett.* **18**(10), 6229–6236 (2018).
22. A. Schmidt et al., "Bacteriophage tailspike protein based assay to monitor phase variable glucosylations in *Salmonella* O-antigens," *BMC Microbiol.* **16**(1), 207 (2016).
23. S. G. Bartual et al., "Structure of the bacteriophage T4 long tail fiber receptor-binding tip," *PNAS* **107**(47), 20287–20292 (2010).
24. G. J. Thomas, Jr. et al., "Conformational stability of P22 tailspike proteins carrying temperature-sensitive folding mutations," *Biochemistry* **29**(17), 4181–4187 (1990).
25. N. Bonilla et al., "Phage on tap—a quick and efficient protocol for the preparation of bacteriophage laboratory stocks," *PeerJ* **4**, e2261 (2016).

26. K. Hodyra-Stefaniak et al., "Mammalian host-versus-phage immune response determines phage fate *in vivo*," *Sci. Rep.* **5**, 14802 (2015).
27. Y. Shao and N. Wang, "Bacteriophage adsorption rate and optimal lysis time," *Genetics* **180**(1), 471–482 (2008).
28. R. H. Edgar, "Evolution of bacteriophage host attachment using Det7 as a model," PhD Thesis, University of Pittsburgh (2014).
29. A. N. Chatterjee, "Use of bacteriophage-resistant mutants to study the nature of the bacteriophage receptor site of *Staphylococcus aureus*," *J. Bacteriol.* **98**(2), 519–527 (1969).
30. S. R. Casjens et al., "Genome sequence of *Salmonella enterica* phage Det7," *Genome Announc.* **3**(3), e00279-15 (2015).
31. P. Meysman et al., "Expression divergence between *Escherichia coli* and *Salmonella enterica* serovar *Typhimurium* reflects their lifestyles," *Mol. Biol. Evol.* **30**(6), 1302–1314 (2013).
32. S. Manohar and D. Razansky, "Photoacoustics: a historical review," *Adv. Opt. Photonics* **8**(4), 586–617 (2016).
33. G. Paltauf, H. Schmidt-Kloiber, and H. Guss, "Light distribution measurements in absorbing materials by optical detection of laser-induced stress waves," *Appl. Phys. Lett.* **69**(11), 1526–1528 (1996).
34. R. A. Kruger et al., "Photoacoustic ultrasound (PAUS)—reconstruction tomography," *Med. Phys.* **22**(10), 1605–1609 (1995).
35. R. M. Weight et al., "Photoacoustic detection of metastatic melanoma cells in the human circulatory system," *Opt. Lett.* **31**(20), 2998–3000 (2006).
36. G. Gutierrez-Juarez et al., "Detection of melanoma cells *in vitro* using an optical detector of photoacoustic waves," *Lasers Surg. Med.* **42**(3), 274–281 (2010).
37. C. M. O'Brien et al., "Capture of circulating tumor cells using photoacoustic flowmetry and two phase flow," *J. Biomed. Opt.* **17**(6), 061221 (2012).
38. M. Leppänen et al., "Imaging bacterial colonies and phage–bacterium interaction at sub-nanometer resolution using helium-ion microscopy," *Adv. Biosyst.* **1**(8), 1700070 (2017).
39. J. L. Castro-Mejía et al., "Optimizing protocols for extraction of bacteriophages prior to metagenomic analyses of phage communities in the human gut," *Microbiome* **3**(1), 64 (2015).
40. K. R. Yamamoto et al., "Rapid bacteriophage sedimentation in the presence of polyethylene glycol and its application to large-scale virus purification," *Virology* **40**(3), 734–744 (1970).
41. M. Mirande, M. Lazard, and J.-P. Waller, "Small-scale purification of bacteriophage λ DNA by an airfuge centrifugation step in cesium chloride gradients," *Gene Anal. Tech.* **5**(4), 80–82 (1988).
42. E. Goldwasser et al., "Physicochemical properties of baeteriophages. iii. Diffusion of bacteriophage T6," *J. Biol. Chem.* **190**(1), 75–81 (1951).
43. G. R. Chase and D. G. Hoel, "Serial dilutions: error effects and optimal designs," *Biometrika* **62**(2), 329–334 (1975).
44. E. Rostova et al., "Kinetics of antibody binding to membranes of living bacteria measured by a photonic crystal-based biosensor," *Biosensors* **6**(4), 52 (2016).
45. K. Butela and J. Lawrence, "Population genetics of *Salmonella*: selection for antigenic diversity," in *Bacterial Population Genetics in Infectious Disease*, D. Ashley Robinson, D. Falush, and Edward J. Feil, Eds., pp. 287–319, John Wiley & Sons, Inc. (2010).
46. P. E. Orndorff, "Use of bacteriophage to target bacterial surface structures required for virulence: a systematic search for antibiotic alternatives," *Curr. Genet.* **62**(4), 753–757 (2016).
47. S. J. Labrie, J. E. Samson, and S. Moineau, "Bacteriophage resistance mechanisms," *Nat. Rev. Microbiol.* **8**(5), 317–327 (2010).
48. J. F. Kreisberg et al., "The interdigitated β-helix domain of the P22 tailspike protein acts as a molecular clamp in trimer stabilization," *Protein Sci.* **11**(4), 820–830 (2002).
49. Institute of Laboratory Animal Resources (US), Committee on Methods of Producing Monoclonal Antibodies, *Monoclonal Antibody Production*, National Academies Press, Washington, DC (1999).
50. W. Wang et al., "Antibody structure, instability, and formulation," *J. Pharm. Sci.* **96**(1), 1–26 (2007).
51. N. B. Hubbs, M. M. Whisby-Pitts, and J. L. McMurry, "Kinetic analysis of bacteriophage Sf6 binding to outer membrane protein a using whole virions," *bioRxiv*, 509141 (2019).
52. J. Landry et al., "Measuring affinity constants of 1450 monoclonal antibodies to peptide targets with a microarray-based label-free assay platform," *J. Immunol. Methods* **417**, 86–96 (2015).

Robert H. Edgar received his MS degree in microbiology from the University of Pittsburgh in 2013 following earlier work at the University of Pittsburgh receiving a MAT in secondary science education as well as a BS degree in biology and BA degree in biblical studies from Geneva College. Currently, he is completing his doctoral work at the University of Pittsburgh Swanson School of Engineering in bioengineering with Dr. John Viator.

Justin Cook is an undergraduate student in biomedical engineering at Duquesne University under a scholarship from the Pennsylvania Junior Academy of Sciences. He intends to enroll in medical school after graduation as a physician-scientist. He has been working in biomedical optics research since he began his undergraduate studies.

Cierra Noel is a graduate of the Biomedical Engineering Program at Duquesne University and is currently an engineering with Westmoreland Mechanical Testing and Research. She was active in bacteriophage research using photoacoustic methods.

Austin Minard is a graduate of the Biomedical Engineering Program at Duquesne University and is matriculated in the graduate program in medical device engineering at the University of Pittsburgh.

Andrea Sajewski is a graduate of the Biomedical Engineering Program at Duquesne University and is a doctoral student in the Department of Bioengineering at the University of Pittsburgh. She is a 2019 recipient of an NSF graduate research fellowship and is currently researching imaging methods using MRI.

Matthew Fitzpatrick was an undergraduate student in the School of Business and the graduate program in biomedical engineering at Duquesne University. He was active in photoacoustic flow cytometry research.

Rachel Fernandez is an undergraduate student in the dual degree program in biomedical engineering and nursing at Duquesne University. She was a corpsman in the US Navy. Currently, she is conducting research in biomedical optics at Duquesne University.

John D. Hempel received his PhD in biochemistry from Rutgers University in 1981, following earlier work at the University of Richmond and a BS degree in biology from William and Mary. He did postdoctoral work in protein structure in Professor Hans Jörnvall's lab at Karolinska Institute in Stockholm, and continued those studies with NIH funding on the structure of aldehyde dehydrogenases at the University of Pittsburgh.

John A. Kellum is an endowed chair in critical care research and vice chair of research in the Department of Critical Care Medicine at the University of Pittsburgh and is a renowned researcher in sepsis and its causes. He is a graduate of the Medical College of Ohio and the University of Toledo.

John A. Viator is the founding chair of the Department of Engineering at Duquesne University and has been conducting research and development of photoacoustic flow cytometry for over a decade. He is a graduate of the University of Washington, the University of Oregon, and Oregon Health and Science University.